Principles and Practice of Urooncology

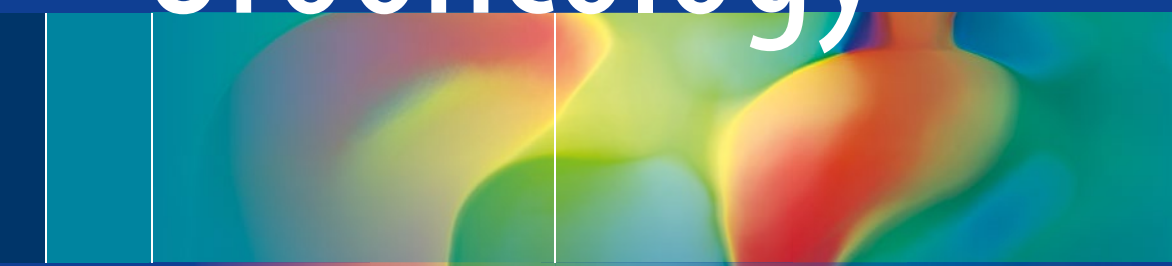

Radiotherapy, Surgery and Systemic Therapy

Gokhan Ozyigit
Ugur Selek
Editors

Springer

Principles and Practice of Urooncology

Gokhan Ozyigit • Ugur Selek
Editors

Principles and Practice of Urooncology

Radiotherapy, Surgery and Systemic Therapy

Springer

Editors
Gokhan Ozyigit
Chair and Professor
Department of Radiation Oncology
Hacettepe University
Ankara
Turkey

Ugur Selek
Chair and Professor
Department of Radiation Oncology
Koc University
Istanbul
Turkey

Adjunct Professor
Department of Radiation Oncology
The University of Texas MD Anderson
Cancer Center
Houston, TX
USA

ISBN 978-3-319-56113-4 ISBN 978-3-319-56114-1 (eBook)
DOI 10.1007/978-3-319-56114-1

Library of Congress Control Number: 2017948435

Printed on acid-free paper

This Springer imprint is published by Springer Nature
The registered company is Springer International Publishing AG
The registered company address is: Gewerbestrasse 11, 6330 Cham, Switzerland

To our families "Eda, Defne, Ipek" and "Ozlem, Melis, Burce," whose supports have made this book possible.
To our patients from whom we have learned to excel.

Preface

This evidence-based guide on lower genitourinary system (GUS) cancers is aiming to be a reference and first-aid book to enable practicing urooncologists to achieve the current management in the multidisciplinary setting of patient selection and cutting-edge treatment finalization.

This guide includes a surgical urooncology perspective with advanced technology to understand the competing surgical approaches, in addition to a medical oncology perspective in multidisciplinary tumor board.

The illustrative spectrum starting from delineation of tumor volumes and organs at risk based on CT simulation and ending at different definitive approaches of stereotactic body radiotherapy (SBRT), intensity-modulated radiation therapy (IMRT), tomotherapy, volumetric modulated arc therapy (VMAT), and proton therapy will highlight the practical tips to ease the management of everyday challenging cases and also provide a comparison of robotic radiosurgical techniques as CyberKnife and LINAC-based techniques.

Each related chapter will display an academic expert view of everyday cases at different stages including case presentations, contouring, treatment planning, and treatment delivery based on illustrations of slice-by-slice delineations on planning CT images and finalization of plan on detailed acceptance criteria. The book will be of value for practicing oncologists as well as other oncology fellows and residents interested in urooncology to facilitate the decision making in the management of patients with lower GUS cancers and will aid encountering daily challenges in clinical practice.

We hope *Principles and Practice of Urooncology* will meet the need for a practical and up-to-date review of lower genitourinary tumors for residents, fellows, and clinicians of radiation and medical and urological oncology, as well as for medical students, physicians, and medical physicists interested in lower genitourinary system malignancies.

Ankara, Turkey — Gokhan Ozyigit, M.D.
Istanbul, Turkey — Ugur Selek, M.D.

Acknowledgments

The editors are indebted to Corinna Hauser and Wilma McHugh from Springer DE and Abha Krishnan and Sivakumar Krishnamoorthy from SPi Global/Springer Nature for their assistance in preparing *Principles and Practice of Urooncology: Radiotherapy, Surgery, and Systemic Therapy*. We extend our most sincere gratitude to our colleagues and friends at Hacettepe University, Koc University, Başkent University, and University of Texas MD Anderson Cancer Center, as well as our families.

Contents

List of Contributors

Omer Acar, M.D. Department of Urology, School of Medicine, Koc University, Istanbul, Turkey

Bülent Akdoğan, M.D. Department of Urology, Hacettepe University, Ankara, Turkey

Sercan Aksoy, M.D. Department of Medical Oncology, Hacettepe University Cancer Institute, Ankara, Turkey

Fadıl Akyol, M.D. Department of Radiation Oncology, Hacettepe University, Ankara, Turkey

Vildan Alpan, M.Sc. Department of Radiation Oncology, American Hospital Texas MD Anderson Cancer Center, Istanbul, Turkey

Mesut Altan, M.D. Department of Urology, Hacettepe University, Ankara, Turkey

Sevil Bavbek, M.D. Department of Medical Oncology, American Hospital, Istanbul, Turkey

Yasemin Bolukbasi, M.D. Department of Radiation Oncology, Koc University, Istanbul, Turkey

Department of Radiation Oncology, The University of Texas MD Anderson Cancer Center, Houston, TX, USA

Seungtaek Choi, M.D. Department of Radiation Oncology, The University of Texas MD Anderson Cancer Center, Houston, TX, USA

Tarık Esen, M.D. Department of Urology, School of Medicine, Koc University, Istanbul, Turkey

Department of Urology, VKF American Hospital, Istanbul, Turkey

Ozan Cem Guler, M.D. Department of Radiation Oncology, Karadeniz Technical University, Trabzon, Turkey

Melis Gultekin, M.D. Department of Radiation Oncology, Hacettepe University, Ankara, Turkey

Pervin Hurmuz, M.D. Department of Radiation Oncology, Hacettepe University, Ankara, Turkey

Muşturay Karçaaltıncaba, M.D. Department of Radiology, Hacettepe University, Ankara, Turkey

Steven Kirsner, Ph.D. Department of Radiation Oncology, The University of Texas MD Anderson Cancer Center, Houston, TX, USA

Deborah A. Kuban, M.D., F.A.C.R., F.A.S.T.R.O. Department of Radiation Oncology, The University of Texas MD Anderson Cancer Center, Houston, TX, USA

Nil Molinas Mandel, M.D. Department of Medical Oncology, VKF Amerikan Hospital, Istanbul, Turkey

Selen Mandel Bezmialem School of Medicine, Istanbul, Turkey

Aydin Mungan, M.D. Department of Urology, Bulent Ecevit University, Zonguldak, Turkey

Cem Onal, M.D. Department of Radiation Oncology, Başkent University, Adana, Turkey

Mehmet Ruhi Onur, M.D. Department of Radiology, Hacettepe University, Ankara, Turkey

Haluk Ozen, M.D. Department of Urology, Hacettepe University, Ankara, Turkey

Gokhan Ozyigit, M.D. Department of Radiation Oncology, Hacettepe University, Ankara, Turkey

Yücel Sağlam, M.Sc. Department of Radiation Oncology, American Hospital Texas MD Anderson Cancer Center, Istanbul, Turkey

Sezin Yuce Sari, M.D. Department of Radiation Oncology, Hacettepe University, Ankara, Turkey

Ugur Selek, M.D. Department of Radiation Oncology, Koc University, Istanbul, Turkey

Department of Radiation Oncology, The University of Texas MD Anderson Cancer Center, Houston, TX, USA

Mehmet Ali Nahit Şendur, M.D. Department of Medical Oncology, Ankara Yıldırım Beyazıt University, Ankara, Turkey

Duygu Sezen, M.D. Department of Radiation Oncology, Koc University, Istanbul, Turkey

Department of Radiology, Hacettepe University, Ankara, Turkey

Ilker Tinay, M.D. Department of Urology, School of Medicine, Marmara University, Istanbul, Turkey

Funda Vakar-Lopez, M.D. Department of Pathology, University of Washington, Seattle, WA, USA

Gozde Yazici, M.D. Department of Radiation Oncology, Hacettepe University, Ankara, Turkey

Berna Akkus Yildirim, M.D. Department of Radiation Oncology, Başkent University, Adana, Turkey

Radiological Imaging in Urological Cancers

1

Mehmet Ruhi Onur and Muşturay Karçaaltıncaba

Abstract

The use of radiological imaging in urological cancers is increasing with improvements in imaging technologies and implementation of these techniques to clinical scenarios. Ultrasonography, computed tomography, and magnetic resonance imaging have enormous potentials in the diagnosis, staging, and surveillance of urological cancers. Emerging imaging techniques enable morphologic assessment of urological cancers with high spatial and contrast resolution. Functional imaging techniques reveal microstructure of tumors which can be used in the diagnosis, prediction of prognosis, and assessment of response to treatment and surveillance of tumors. Biopsyless diagnosis may be possible in the future particularly for renal and prostate tumors. In this chapter, current status of urooncologic imaging will be reviewed.

1.1 Introduction

Urological cancers constitute one of the most frequent encountered malignancies in urologic and oncologic practice. Imaging has a critical role in the diagnosis of urological tumors as well as staging and active surveillance. In addition to the morphologic and functional assessment of tumors, imaging techniques can be used to guide the interventional procedures including biopsy, preoperative embolization, or ablation providing palliative care or curative treatment. Optimal evaluation and treatment of urological cancers can be accomplished with appropriate use of imaging techniques for the diagnosis and staging of tumors, guidance for invasive procedures, and active surveillance of patients.

M.R. Onur, M.D. • M. Karçaaltıncaba, M.D. (✉)
Department of Radiology, Hacettepe University, Ankara, Turkey
e-mail: musturayk@yahoo.com

G. Ozyigit, U. Selek (eds.), *Principles and Practice of Urooncology*,
DOI 10.1007/978-3-319-56114-1_1

Ultrasonography (US) is usually the first preferred imaging technique in the diagnosis of urological cancers. As a noninvasive, inexpensive, easily accessible, and nonionizing radiation used imaging method, US can be used in patients as a first-step imaging technique in patients with suspected malignancy. US demonstrates solid and/or cystic content of the urological masses. Color-flow Doppler US (CDUS) can reveal blood flow within the mass. However grayscale US and CDUS have remarkable limitations in characterization of urological masses. Contrast-enhanced US (CEUS) can demonstrate the enhancement features of tumors which increase the likelihood of neoplastic nature of a mass and can be used in differentiation between benign and malignant urological masses. New emerging technologies promise increased capability for detection and characterization of urological cancers.

Computed tomography (CT) is the mainstay imaging technique utilized in radiologic assessment of renal, ureteral, and bladder cancers. With its multiplanar imaging capability acquired in a short scanning time, CT can demonstrate morphological imaging features, attenuation values, and contrast enhancement patterns of tumors. CT may be helpful to characterize urological cancers by comparison of density values of urological cancers represented by Hounsfield unit (HU) at unenhanced, early, and delayed phases after intravenous (IV) contrast administration.

Magnetic resonance imaging (MRI) is a problem-solving imaging technique in the radiologic assessment of urological cancers. Acquisition of multiple imaging sequences with high soft tissue contrast resolution assigns MRI as decision-making technique in difficult cases. Multiparametric MRI (mp-MRI) technique which consists of conventional MRI sequences such as T1-weighted (W), T2-W, dual-echo T1-W sequences combined with functional MRI sequences including diffusion-weighted imaging (DWI) and dynamic contrast-enhanced MRI (DCE-MRI) are being more increasingly used in detection and characterization of the urological cancers.

1.2 Renal Cancer

1.2.1 General Information

Renal cancers account for 3% of adult malignancies, occurring at a mean age of 65. Male predominance exists in renal cancers with a male to female ratio of 3:1 [1]. Renal cancers are more frequently detected at early stages due to frequent incidental presentation of renal tumors on cross-sectional imaging studies performed due to indications other than urological symptoms. The likelihood of malignancy is 80% in all solid renal lesions detected on imaging studies [2]. However 38% of renal lesions less than 1 cm are benign [3]. Detection of renal tumors on imaging studies necessitates differentiation between benign and malignant masses. In the setting of renal malignancy assessment of other kidney in terms of renal mass is mandatory since 5% of sporadic renal tumors present as bilateral multifocal renal masses [4, 5].

Best prognostic factors in renal cancers are grade and stage of the cancers determined with Fuhrman grading system and tumor-node-metastasis (TNM) staging system, respectively. Fuhrman grading system classifies renal carcinomas according to nuclear size and shape and the size of the nucleoli [1]. TNM staging system includes localization of renal cancers, extension of tumors to perirenal tissues, and metastatic involvement of lymph nodes and distant tissues and organs. Imaging techniques can determine the local and distant spread of renal cancers.

1.2.2 Imaging Techniques

1.2.2.1 Ultrasonography

Ultrasonography is helpful for initial screening of renal lesions as well as to discriminate cystic lesions from solid lesions and monitoring growth of previously determined lesion [6]. Renal cancers usually present as a focal, expansile mass with heterogeneous echogenicity different from adjacent hypoechoic renal parenchyma. Heterogeneous echogenicity and expansile nature of renal cancers are helpful in distinguishing renal cancers from pseudotumoral renal lesions such as column of Bertin and dromedary hump of the kidney. However detection of small renal cancers (<3 cm) confined in renal parenchyma without expansile appearance may be difficult with US especially if these cancers have isoechoic appearance similar to renal parenchyma. Renal cell carcinoma (RCC) as being most frequently encountered renal tumor usually manifests as hypo-, iso-, or hyperechoic expansile mass on US (Figs. 1.1 and 1.2).

Small renal masses (<3 cm) may more likely present with hyperechoic appearance than larger tumors [7]. Papillary RCCs usually appear as hypoechoic or isoechoic and rarely hyperechoic solid masses (Fig. 1.3) [8]. However it is nearly

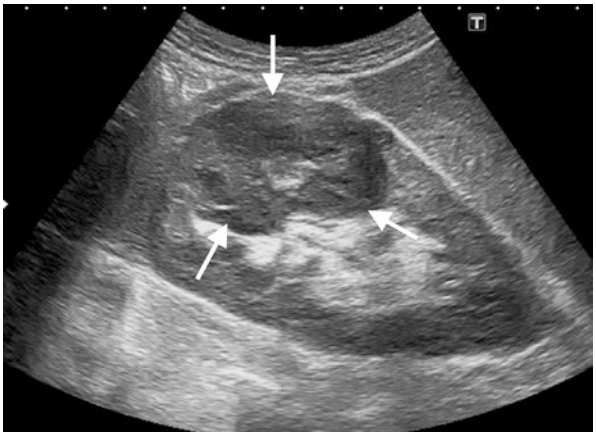

Fig. 1.1 Clear cell RCC. Grayscale US of a 78-year-old male demonstrates a hypoechoic expansile solid renal mass (*arrows*)

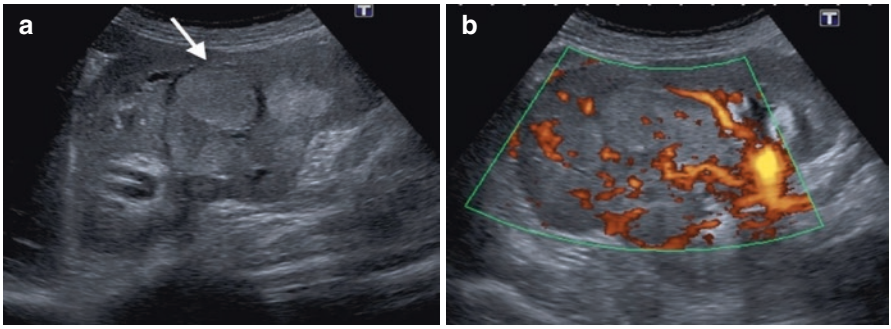

Fig. 1.2 Chromophobe RCC. (**a**) Grayscale US of a 56-year-old female with chromophobe RCC reveals multilobulated hyperechoic solid mass (*arrow*). (**b**) Power Doppler US demonstrates hypervascularity of the tumor

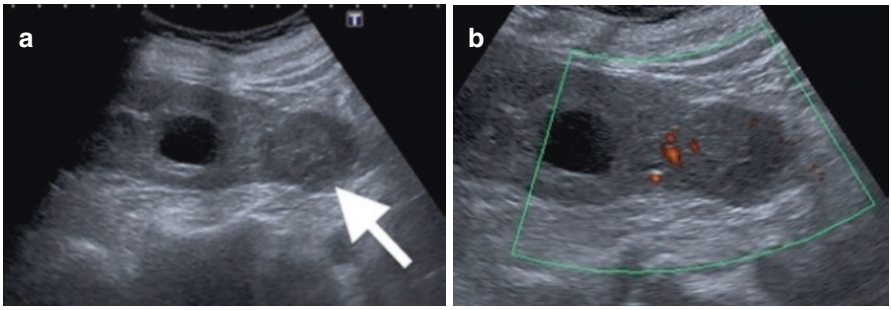

Fig. 1.3 Papillary cell RCC. (**a**) Grayscale US of a 66-year-old male with papillary RCC shows hypoechoic renal mass (*arrow*) arising from lower pole of the kidney and extending inferiorly. (**b**) Renal mass presents with low vascularity on power Doppler US

impossible to differentiate subtypes of RCCs such as clear cell RCC, papillary RCC, and chromophobe RCC by US due to similar sonographic features of these tumors on grayscale US and CDUS. Generally, papillary cell types of RCCs have less vascularity compared to other types of RCCs on CDUS (Fig. 1.3). Renal lymphomas and metastases may manifest as multifocal infiltrative masses (Fig. 1.4). Renal pelvis tumors, most frequently as transitional cell carcinomas (TCCs), present with a hypoechoic appearance within the hyperechoic renal sinus (Fig. 1.5). However TCCs or other tumors localized in renal pelvis are usually more susceptible to be missed on US compared to renal parenchymal tumors.

Cystic renal masses detected on US should be elaborated in terms of malignancy. Sonographic features that increase the likelihood of malignancy in complex renal cysts include thickened cyst wall, numerous or thickened or nodular septations within the cyst, presence of irregular or central calcifications, and the presence of blood flow in the septations or cyst wall (Fig. 1.6) [9]. US can be an important complementary method by revealing cystic nature of hyperdense,

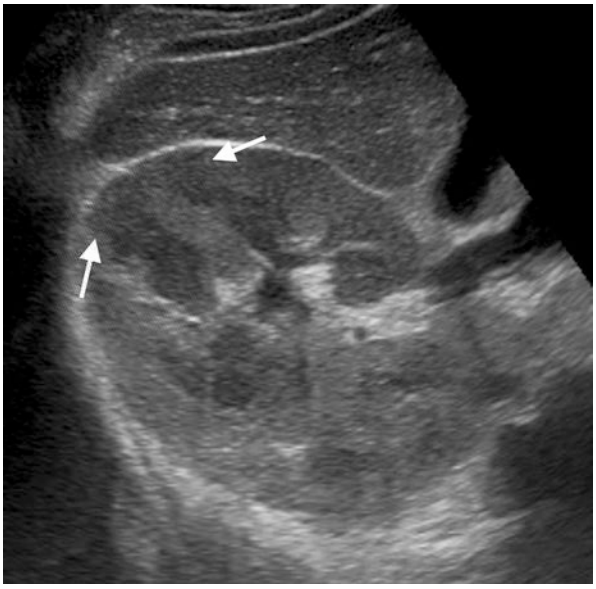

Fig. 1.4 Renal lymphoma. Grayscale US reveals multifocal hypoechoic infiltrative lesions (*arrows*) in the renal parenchyma representing lymphomatous involvement

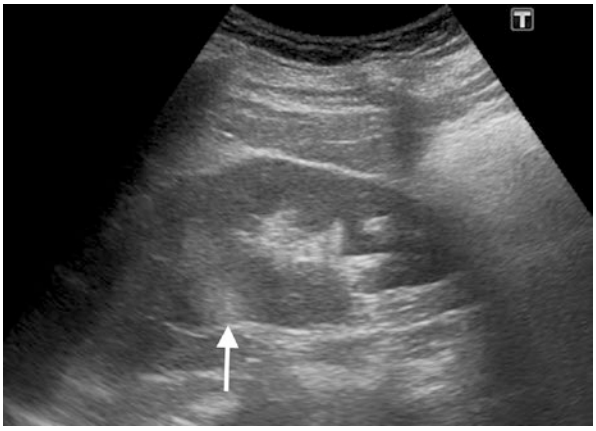

Fig. 1.5 Renal TCC. Grayscale US of a 72-year-old female with TCC demonstrates a hypoechoic solid mass (*arrow*) in the renal pelvis replacing hyperechoic renal sinus fat in the upper pole of the kidney

solid-appearing renal lesions on CT and solid nature of lesions which appear as cystic mass on CT [10].

Contrast-enhanced US seems to be a promising imaging technique for distinguishing benign and malignant renal tumors. A meta-analysis study including

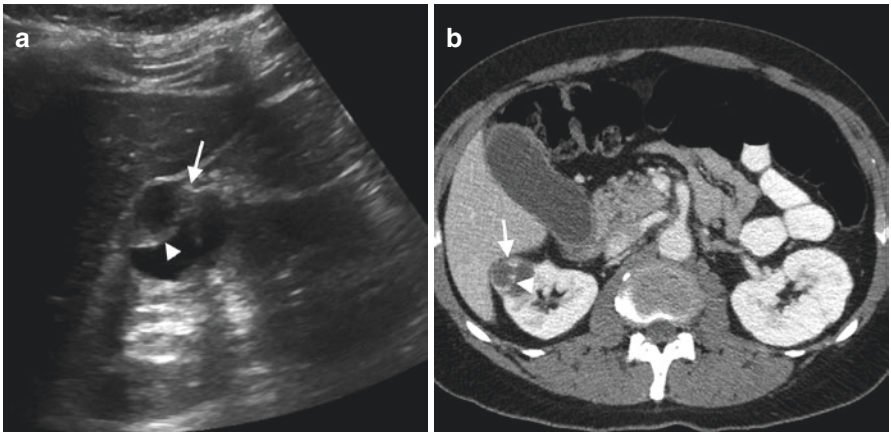

Fig. 1.6 Cystic RCC. (**a**) Grayscale US reveals cystic renal mass (*arrow*) containing thick septa (*arrowhead*). (**b**) Axial contrast-enhanced CT reveals cystic renal mass (*arrow*) in the right kidney with enhancing septa (*arrowhead*)

11 studies reported a pooled sensitivity of 88% and specificity of 80% in differentiation between benign and malignant renal tumors by CEUS [11].

Ultrasound elastography is an emerging technique based on measuring elasticity of biological tissues by calculating their response to manually applied force by US probe or propagating sound waves. Since malignant renal tumors are assumed to be stiffer than benign tumors, it has been suggested that US elastography can be used to differentiate benign and malignant renal tumors (Fig. 1.7). Although successful results imply the utility of US elastography in differentiation between benign and malignant renal tumors, determination of subtypes of renal tumors seems to be unpredictable by this technique [12].

Assessment of renal vein involvement is mandatory in case of renal cancers. Renal veins should be visualized from renal hilum to inferior vena cava (IVC) on CDUS to detect hypo- or hyperechoic filling defect with solid appearance in renal vein representing tumoral thrombus. CDUS is comparable to MRI for detecting tumoral extension to renal veins and inferior vena cava with a sensitivity of 86% and specificity of 94% [13–15].

Main limitation of US in assessment of renal tumors is difficulty to detect and characterize small renal masses. One study showed that 42% of renal lesions between 15 and 20 mm were not detected on US while CT detected 100% of lesions [16]. User dependency which may cause interobserver variability in follow-up of lesions is another limitation of US.

Intraoperative US yields high-resolution images in partial nephrectomies and enucleation of tumors. Intraoperative US can demonstrate new findings which were not detected on preoperative imaging in 10.6% of cases and alters the surgical management in 71.4% of patients with renal cancers [17].

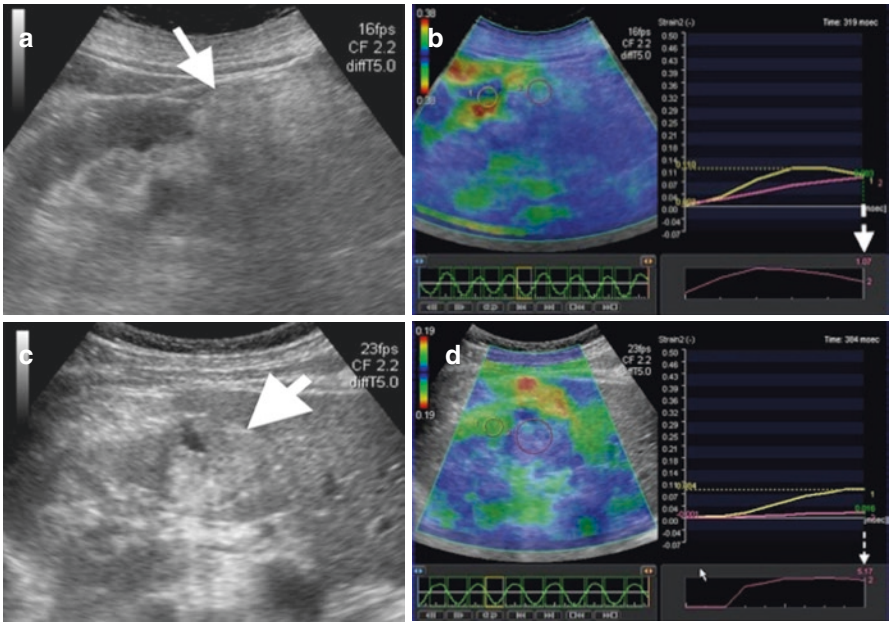

Fig. 1.7 Ultrasound elastography of renal masses. (**a**) Grayscale US image of a 48-year-old female demonstrates hyperechoic mass (*arrow*) representing angiomyolipoma. (**b**) Strain elastography of the mass depicts strain index value as 1.07 (*dashed arrow*) corresponding to benign renal mass. (**c**) Grayscale US image of a 55-year-old male with RCC reveals hyperechoic solid mass (*arrow*) in the kidney. (**d**) Strain elastography depicts strain index value of the mass as 5.17 (*dashed arrow*) representing increased stiffness and likelihood of malignancy of the mass

1.2.2.2 Computed Tomography

Computed tomography is the decision-making imaging technique in assessment of renal tumors. Awareness of sonographic imaging features of renal mass may be helpful for planning CT protocol since renal parenchymal or pelvis tumors should be scanned with different CT protocols. The use of intravenous (IV) iodinated contrast material and ionizing radiation in CT examination mandates appropriate planning of CT protocol. Multiphasic CT protocols used in the evaluation of renal mass include precontrast scanning and corticomedullary (scan delay 35–40 s after IV contrast injection), nephrographic (scan delay 70–90 s after IV contrast injection), and delayed excretory (scan delay 5–10 min after IV contrast injection) phases [18]. Precontrast images demonstrate calcifications in the renal masses and yield a baseline density measurement to compare enhancement degree and pattern of the tumors on contrast-enhanced images. Precontrast CT is also critical in depicting hypovascular hemorrhagic cysts which may be misdiagnosed on contrast-enhanced images as hypovascular papillary RCC [19]. In these cases, unenhanced CT demonstrates hyperdense appearance of hemorrhagic cysts secondary to high attenuation of the

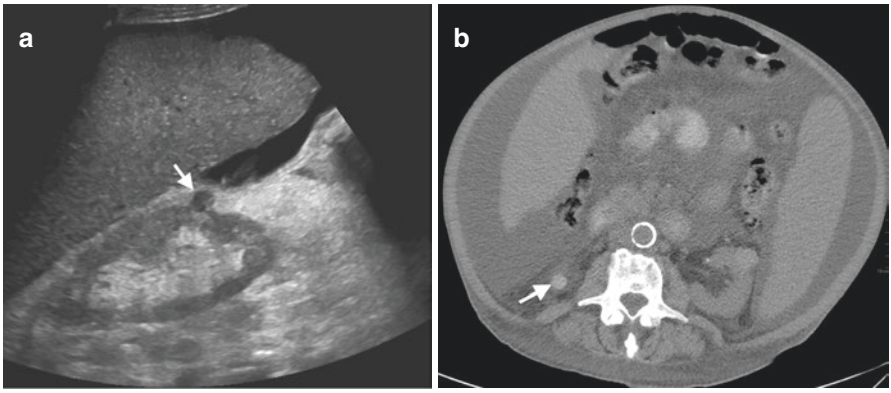

Fig. 1.8 Hemorrhagic cyst. (**a**) Grayscale US image of a 45-year-old female shows well-circumscribed hypoechoic cyst-like mass (*arrow*) located near the lower pole of the right kidney. The absence of posterior acoustic enhancement suggests probability of solid mass. (**b**) Precontrast axial CT image reveals hyperattenuation in the mass (*arrow*) representing hemorrhagic cyst

blood on CT and helps to realize pseudoenhancement of hemorrhagic cysts on contrast-enhanced CT images (Fig. 1.8). Corticomedullary images demonstrate lesion vascularity and renal vascular anatomy. Renal cortex enhances more than renal medulla in corticomedullary phase. Images acquired on this phase may help to distinguish hypervascular clear cell carcinoma from hypovascular papillary cell carcinoma [19]. However renal masses localized in renal medulla may be missed on corticomedullary phase images. In nephrographic phase renal parenchyma enhances homogeneously with similar enhancement in renal cortex and medulla. Renal tumors manifest as less enhancing solid or semisolid lesions compared to renal parenchyma (Fig. 1.9). This phase is the most helpful imaging phase for detection and characterization of renal masses [20]. Nephrographic phase images have superiority in detection especially small (<3 cm) renal masses in the renal parenchyma [18]. Excretory images are helpful to delineate renal collecting systems, ureters, and bladder with tumoral involvement of these structures (Fig. 1.9).

Malignant potential of a renal mass increases with presence of significant enhancement which is defined as an attenuation increase of at least 15–20 HU on postcontrast images with respect to the precontrast image [20]. Enhancement of a lesion up to 10 HU is defined as pseudoenhancement which may be encountered in some renal cysts. Enhancement of 10–20 HU in a renal mass on CT refers to indeterminate mass that necessitates assessment with MRI. Other scanning phases give additional valuable information for presurgical planning. Contrast enhancement characteristics of renal masses can be a distinguishing feature in prediction of subtypes of RCCs. Conventional type or clear cell type of RCC as being most frequently detected RCC subtype presents usually as well-circumscribed, heterogeneous mass containing usually two components as solid hypervascular portion and necrotic or hemorrhagic necrotic, avascular portion [21]. Typical clear cell RCC manifests with intense enhancement in the corticomedullary phase and less enhancement

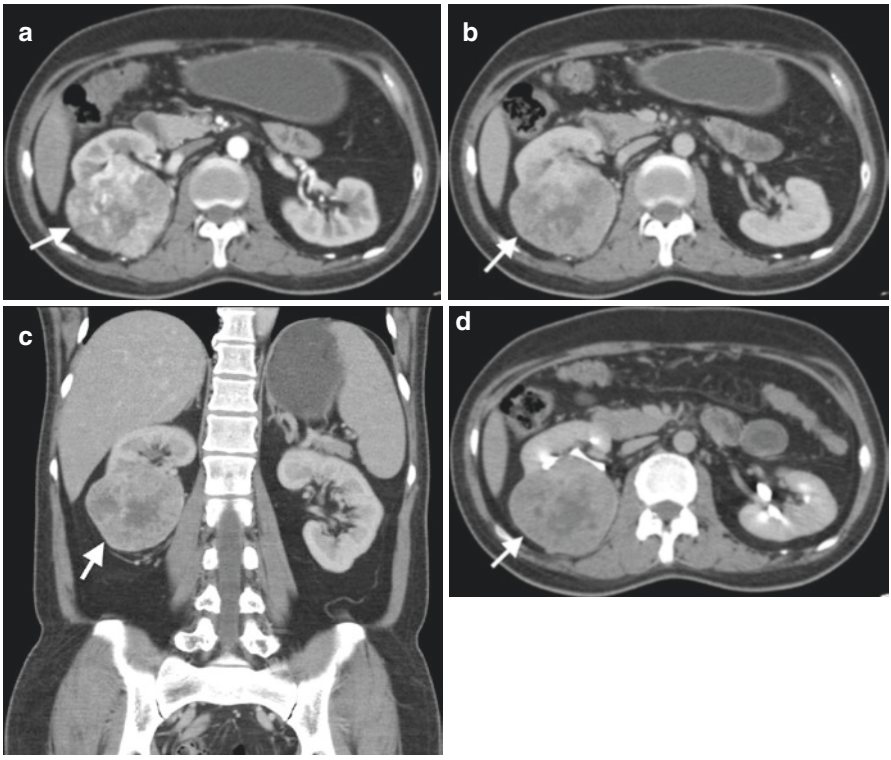

Fig. 1.9 Multiphasic CT of clear cell RCC. (**a**) Axial CT image obtained at corticomedullary phase reveals hypervascular solid mass (*arrow*) arising from the inferior pole of the right kidney. (**b**) Axial and (**c**) coronal CT images at nephrogram phase demonstrate solid mass (*arrows*) enhancing less than adjacent renal parenchyma. (**d**) Axial excretory phase CT image reveals splaying of inferior collecting system by the mass (*arrow*)

compared to renal parenchyma at nephrographic phase. Papillary RCCs were reported as homogeneously enhancing renal mass in comparison to renal parenchyma and other subtypes of RCC [22, 23]. A hypovascular solid renal mass without fat content usually suggests papillary RCC as 82% of the cases manifest with less than or equal to 40 HU enhancement [24].

Small renal lesions which are smaller than 10 mm constitute a challenge for both urooncologists and radiologists. Characterization of renal masses less than 1 centimeter is frequently difficult on CT [21]. If a renal parenchymal lesion appears hypodense compared with the renal cortex on precontrast CT images with the density values of <10 HU or <−20 HU regardless of density values after IV contrast administration, these lesions can be assumed to be a benign renal parenchymal lesion mostly renal cortical cyst and small angiomyolipoma, respectively [21]. When density measurement of small renal parenchymal lesions does not yield any informative value, these lesions can be defined as "indeterminate microlesion, with no suspect characteristics" and can be followed up with imaging [21].

Cystic renal masses detected on CT should be interrogated in terms of malignancy. Bosniak classification system is widely accepted as a reliable tool to define complicated cystic renal masses for likelihood of malignancy. Although Bosniak classification was firstly introduced as CT classification system, the classification scheme may also be applied to MRI [25]. According to Bosniak classification system, category I lesions refer to simple cysts. Category II lesions have smooth septa and minimal wall thickening. Category I and II lesions are benign lesions requiring no further workup. Category IIF lesions include well-marginated cysts with enhancing or nonenhancing multiple hairline-thin septa and nonenhancing high-attenuation renal lesions. These lesions are indeterminate moderately complicated cystic renal masses that require follow-up to demonstrate stability. Category III lesions have thickened wall or septa and include some imaging features suspicious of malignancy that may be managed surgically. The presence of solid component in cystic renal mass refers to Bosniak category IV lesion and indicates high suspicion for malignancy (Fig. 1.10). Category IV lesions are managed surgically. Pseudoenhancement which is characterized as increased density in the cyst wall or septa after IV contrast administration is a pitfall that can cause misdiagnosis of cystic renal malignancy. Pseudoenhancement of cystic renal masses results from volume averaging and beam-hardening effects on CT [22]. Smaller renal cysts tend to be more amenable to pseudoenhancement [26]. Hemorrhagic cysts can present with pseudoenhancement; however hyperdense appearance of hemorrhagic cysts on precontrast CT is characteristic for hemorrhagic cysts.

CT can easily identify macroscopic fat in renal masses. The diagnosis of angiomyolipoma can be established safely on CT when the density of a mass measured as <−20 HU with no content of calcification or necrosis [21]. However RCCs may rarely present with fat component. Fat content in a RCC mostly occurs in papillary cell type [27]. In the setting of fat-containing renal mass, the possibility of

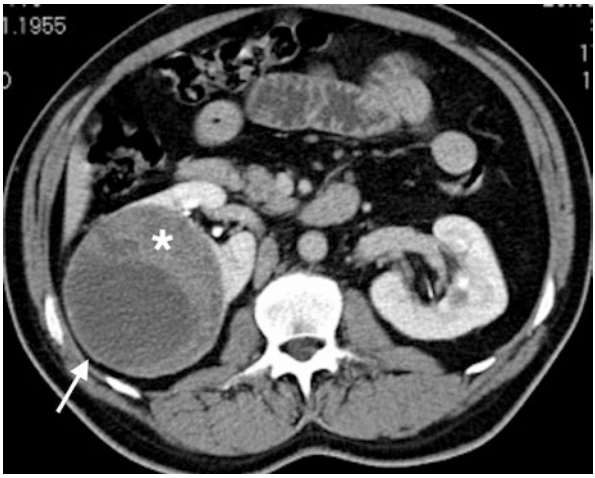

Fig. 1.10 Cystic RCC. Axial contrast-enhanced CT demonstrates cystic mass (*arrow*) with enhancing solid component (*asterisk*) classified as Bosniak category IV and surgically proved to be RCC

malignancy should be thought if a large, solid, infiltrating, and heterogeneous lesion is detected on CT. Calcifications may be encountered in 30% of RCCs which are typically central and irregular [21]. Invasion of the renal vein and inferior vena cava (IVC) occurs in 23% and 7% of RCCs, respectively [28] (Fig. 1.11).

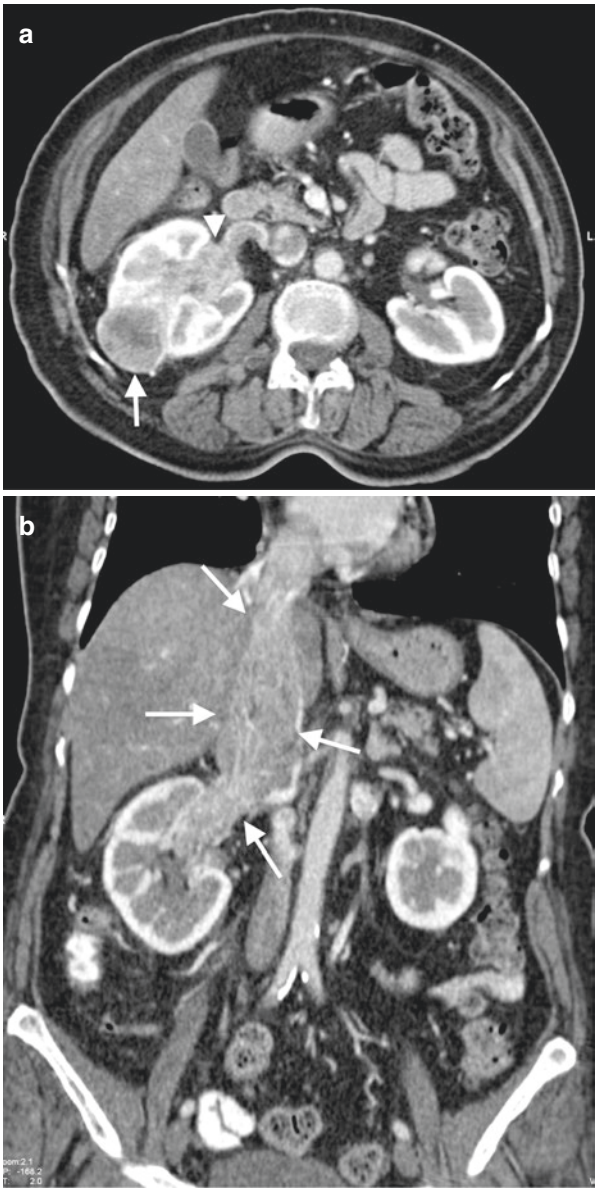

Fig. 1.11 RCC with venous invasion. (**a**) Axial contrast-enhanced CT of a 66-year-old female with RCC demonstrates a solid renal mass (*arrow*) in the interpolar region of the right kidney and invasion of the renal vein with tumor (*arrowhead*). (**b**) Coronal contrast-enhanced CT reveals tumoral invasion of the right renal vein and extension of the tumor thrombus to the right atrium through IVC (*arrows*)

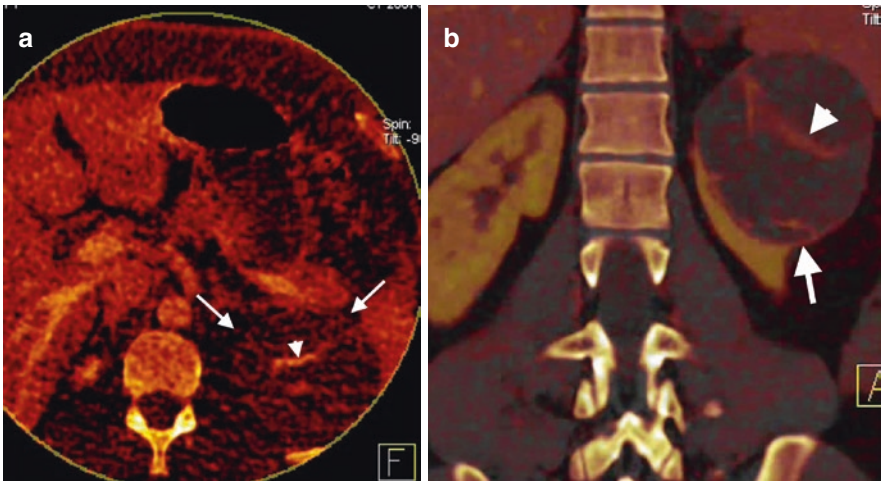

Fig. 1.12 Dual-energy CT of renal mass. Axial iodine overlay (**a**) and coronal mixed (**b**) images of DECT reveal a cystic mass (*arrows*) at the upper pole of the left kidney with a septum formation that uptakes iodine (*arrowhead*)

RENAL nephrometry scoring system is a numerical scoring system of imaging features of renal mass on CT or MRI including maximal tumor radius, exophytic versus endophytic nature of the tumor, relationship of the tumor to the collecting system or sinus, location relative to polar lines, and anterior or posterior tumor location [20]. It was reported that RENAL nephrometry scoring system can be used as a predictor of surgical outcomes of laparoscopic partial nephrectomy and histology and grade of RCCs [29].

Dual-energy CT (DECT) is an evolving CT technology, which is characterized by simultaneous acquisition of CT data with two different energies or peak tube voltages [30]. In this technology different tissues in the organs can be separated by attenuation difference behavior at two different tube voltage levels. Virtual unenhanced CT images can be acquired which contributes to decreasing ionizing radiation dose up to 47% compared to multiphasic CT examination [31]. Iodine content of the renal masses instead of attenuation values (HU) after IV contrast administration can be measured with this technique (Fig. 1.12). DECT can also be helpful to demonstrate pseudoenhancement of renal masses [32].

1.2.2.3 Magnetic Resonance Imaging

Magnetic resonance imaging (MRI) is a problem-solving tool in characterizing renal tumors with its high soft tissue contrast and multiplanar imaging capabilities [33]. MRI can depict water and fat content of renal tumors. Benign and malignant renal tumors may be more accurately differentiated by MRI due to capability of obtaining various sequences which enable to determine fat and water content of renal masses. MRI was shown to be better in evaluating renal lesions which were previously deemed indeterminate on CT [34].

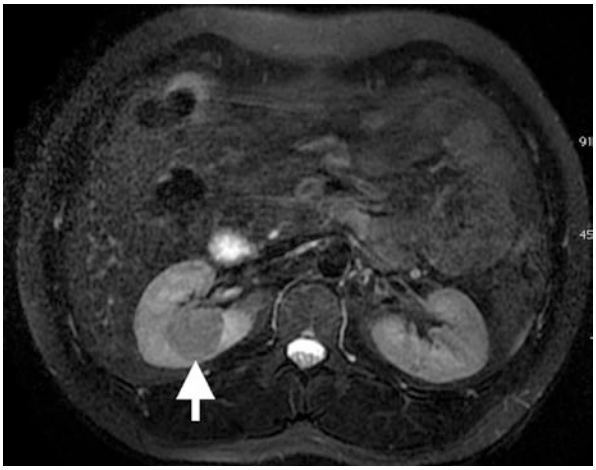

Fig. 1.13 Papillary RCC. Axial T2-W MRI of a 72-year-old male demonstrates a well-circumscribed hypointense mass (*arrow*) in the right kidney

Renal mass evaluation with MRI should include T1-W axial in- and out-of-phase gradient-echo sequence to identify macroscopic and microscopic fat, T2-W axial and coronal sequences to evaluate overall anatomy, renal collecting system, and complexity of cystic renal lesions and dynamic contrast-enhanced (DCE) T1-W fat-suppressed sequences consisting of corticomedullary, nephrographic, and excretory phases. Renal tumors usually appear hypointense on T1-W and hyperintense on T2-W images, while papillary cell RCCs manifest as hypointense lesions on T2-W images (Fig. 1.13). Cystic renal masses can be more easily and accurately characterized by MRI compared to CT. The presence and thickness of septa, wall thickness, and contrast enhancement patterns of renal cystic lesions can be depicted on DCE-MR images. Coronal T1-W images at excretory phase with administration of diuretics can delineate collecting system and ureters and may be helpful in the diagnosis of TCCs.

DWI technique is increasingly used in the assessment of renal tumors. Solid renal tumors demonstrate increased signal intensity on DW images and decreased signal intensity on ADC maps secondary to restricted diffusion of water molecules in renal tumors (Fig. 1.14). DWI has potential to discriminate malignant renal tumors from benign tumors with ADC measurements. It was shown that malignant renal masses have lower ADC values than benign renal masses (Fig. 1.15) [19]. The ADC values of clear cell RCC were shown to be significantly higher than chromophobe and papillary cell RCC which may be helpful to differentiate these subtypes of RCC [35, 36].

Superiority of MRI over other imaging techniques is most remarkable on renal cystic masses with high protein content and hemorrhage. Since these lesions demonstrate high density on precontrast images and may show pseudoenhancement on contrast-enhanced CT images, their diagnosis may be difficult on MDCT.

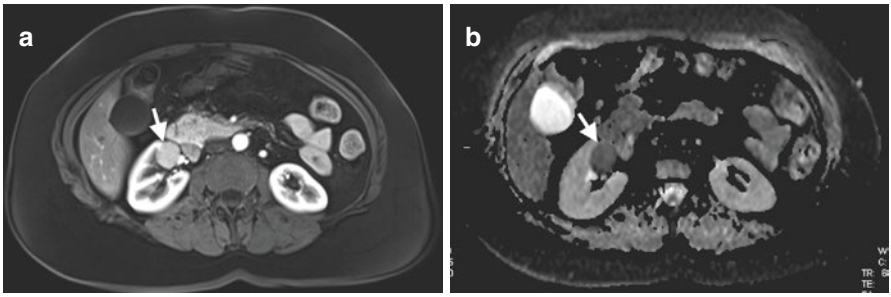

Fig. 1.14 DWI of renal cancer. (**a**) Contrast-enhanced T1-W MRI of a 62-year-old male with chromophobe RCC demonstrates enhancing solid mass (*arrow*) in the right kidney. (**b**) Renal mass presents with signal loss (*arrow*) secondary to restricted diffusion on ADC map

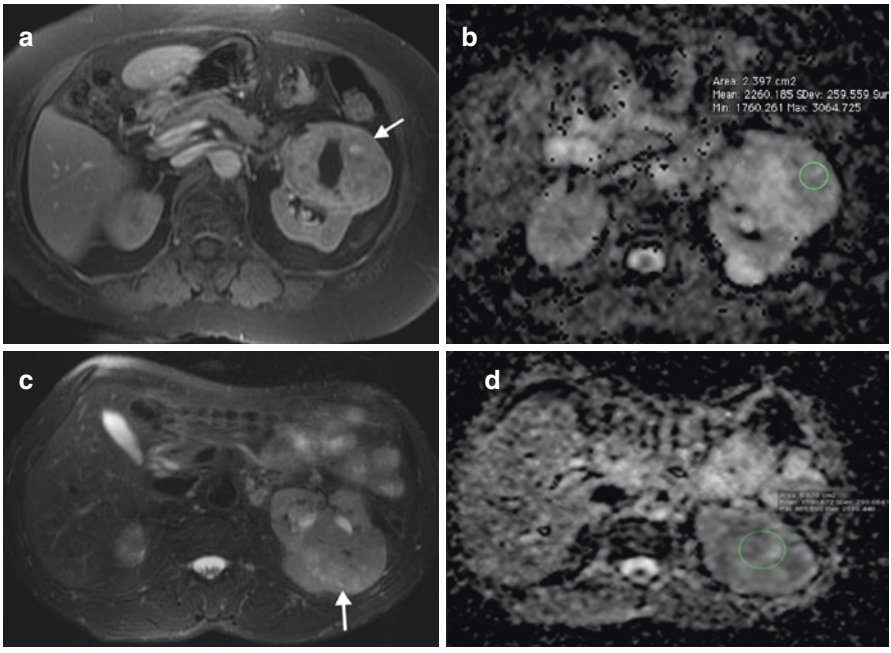

Fig. 1.15 ADC values of benign and malignant renal masses. (**a**) Axial contrast-enhanced fat-saturated T1-W image of a 44-year-old female with oncocytoma reveals enhancing solid mass (*arrow*) with nonenhancing central scar. (**b**) ADC value of the mass on ADC map image is measured as 2.26 mm^2/s. (**c**) Axial T2-W image of a 66-year-old male with chromophobe RCC reveals a hyperintense solid mass (*arrow*) arising from the left kidney. (**d**) ADC value of the mass on ADC map image is measured as 1.59 mm^2/s

MRI provides a solution for this problem with subtraction technique. With MRI subtraction technique, precontrast MR image of a T1-W hyperintense lesion can be subtracted from contrast-enhanced image of same lesion (Fig. 1.16). MRI was shown to be superior than CT on depicting additional septa, thickening of the wall

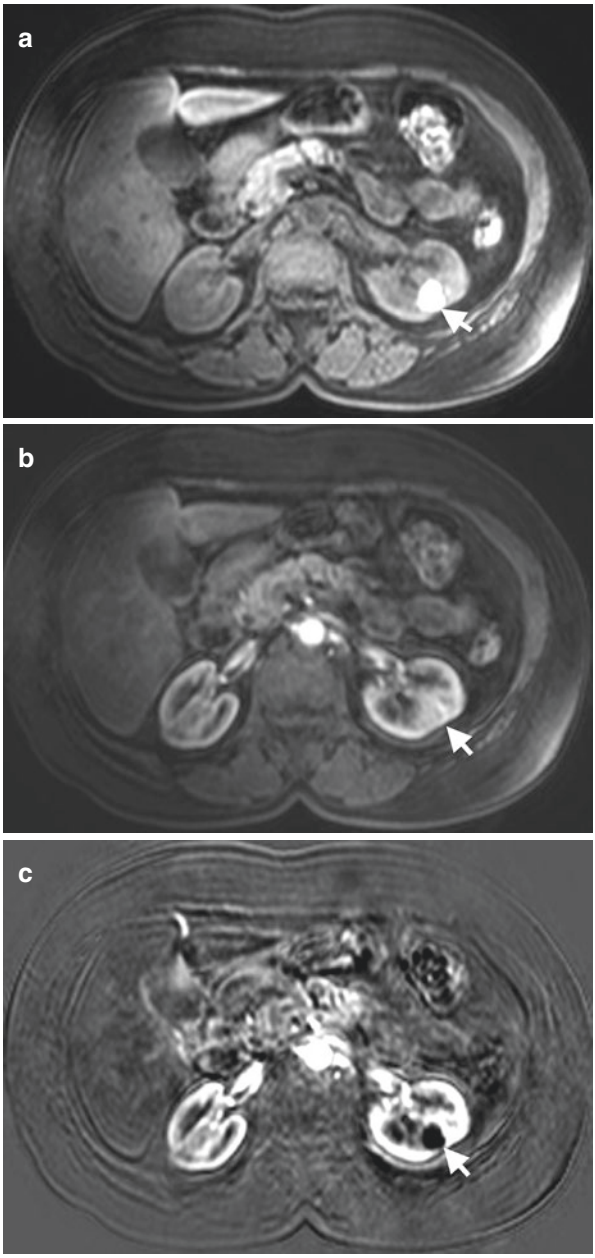

Fig. 1.16 Renal complex cyst on subtraction MRI. (**a**) Axial fat-suppressed T1-W image shows a hyperintense mass (*arrow*) in the left kidney. (**b**) Axial contrast-enhanced T1-W image demonstrates left kidney mass with hyperintense appearance (*arrow*) suggesting contrast enhancement. (**c**) Subtraction image reveals signal loss (*arrow*) in the mass confirming nonenhancement of the mass

or septa, or enhancement of the complex renal cysts [25]. Application of Bosniak criteria to cystic lesions on MRI may lead to upstaging of lesions in 10% of cases which were previously categorized on CT [25].

MRI is also a key imaging tool for differentiation between fat-poor angiomyolipomas (AMLs) from RCC. A study using combination of MR sequences reported sensitivity, specificity, and accuracy values of 73%, 99%, and 96%, respectively, in distinguishing AML from RCC [37].

Multiparametric MRI (mp-MRI) of the kidney refers to acquisition of DCE-MRI, DWI, and perfusion MRI for evaluation of renal tumors. Perfusion MRI techniques including arterial spin labeling (ASL) and blood-oxygen-level-dependent (BOLD) MRI were reported to be helpful in distinguishing between benign and malignant renal masses with the capability of obtaining high-temporal-resolution images compared to conventional dynamic MRI. ASL is characterized by using the endogenous contrast properties of arterial blood and noninvasively labeling inflowing spins without exogenous contrast material administration [38]. ASL was shown to be helpful in distinguishing between RCC and oncocytomas as well as between papillary RCCs from other subtypes of RCC [38, 39]. BOLD MRI may be helpful for distinguishing RCCs from AMLs at 3 T MRI and for differentiation between benign cystic lesions from RCCs [40].

Although gadolinium-based contrast agents that are used in MRI were thought as safe contrast agents before, it is well known that these patients especially ones with impaired kidney function are at the risk of nephrogenic systemic fibrosis. Therefore, the use of gadolinium contrast in patients with low glomerular filtration rate (<30 mL/min/1.73 m^2) is not recommended according to guidelines of American College of Radiology unless risk-benefit assessment favors the use of gadolinium contrast agent [20].

Malignant Tumors of Renal Pelvis

Transitional cell carcinomas and squamous cell carcinomas (SCC) represent 90% and 10% of pelvicalyceal malignant tumors (PMTs), respectively [41]. TCC may present as multifocal, synchronous, or metachronous lesions, which necessitate evaluation of all urinary tract with cross-sectional imaging studies. Computed tomography urography (CTU) enables evaluation of pelvicalyceal system of the kidneys, ureters, and bladder.

PMT manifest as focal mass or thickening of the wall of the urinary tract. US may not detect PMT presenting with thickening of the pelvis or ureteral wall. However focal mass forming PMT can be visualized on US as hypoechoic mass replacing hyperechoic renal sinus fat (Fig. 1.5).

CTU is essential for evaluating PMT especially for detection of synchronous lesions in the entire urinary tract. Mean attenuation value of these tumors (30 HU) is different from water (mean HU, 0), blood clot (mean HU, 50–75), and calculi (mean HU >100) [42]. PMTs enhance mildly or moderately on arterial phase images and manifest with washout on delayed phase images on CT [43]. Renal pelvis tumors most frequently manifest as filling defect in the renal pelvis at excretory

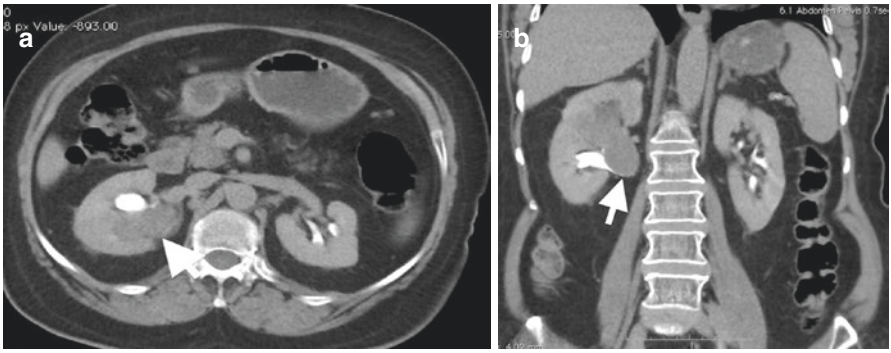

Fig. 1.17 Transitional cell carcinoma of renal pelvis. Axial (**a**) and coronal (**b**) CTU excretory phase images of a 74-year-old male reveal filling defect at the inferior portion of the renal pelvis and calyces caused by solid mass (*arrows*)

phase images (Fig. 1.17). Superficial TCCs can be diagnosed based on the CT features as focal or diffuse mural thickening, focally obstructed calyces, or sessile filling defects within the hyperdense pelvicalyceal system or ureters filled with iodinated contrast material. Renal collecting system may be expanded, and renal fat sinus may be compressed due to mass effect of the PMT. Renal parenchymal invasion may be observed on aggressive and advanced stage of TCC that represents 15% of these tumors and can mimic renal parenchymal malignancies invading renal collecting system [43]. Renal parenchymal invasion of PMT can be defined as obliterated renal sinus fat plane between the mass and renal parenchyma on CT. TCC is more likely to be located centrally and expand the kidney centrifugally with less likely causing contour irregularities compared to RCC invading renal collecting system [44]. CT may play an important role in staging of PMT; however it cannot distinguish T1 tumor (limited to uroepithelium and lamina propria) from T2 tumor (tumor invading the muscularis propria) [22]. Early-stage PMT (T1 and T2) can be distinguished from advanced-stage tumors such as T3 (invading peripelvic fat or renal parenchyma) and T4 (invading adjacent organs or abdominal wall or extending perinephric fat) [22].

Metastases

Renal metastases usually manifest as bilateral and multifocal masses. If a solid renal mass is detected in a patient with extrarenal malignancy and metastases in other organs, probability of the diagnosis of renal metastasis is more likely [45]. However in the absence of other organ metastasis, a solid renal mass is less likely to be a metastasis even in the setting of primary extrarenal malignancy [46]. Renal metastases frequently appear as more infiltrative and less vascular masses compared to clear cell RCCs in the renal parenchyma. Differentiation between primary renal malignancies and metastases is usually difficult according to imaging features on cross-sectional imaging which often necessitate biopsy of the mass in the setting of solitary solid renal mass in patients with extrarenal primary malignancy.